Theor. Appl. Climatol. 76, 189–202 (2003)
DOI 10.1007/s00704-003-0011-x

Theoretical and Applied Climatology

Printed in Austria

[1] The Open University of Israel, Tel-Aviv, Israel
[2] Department of Geophysics and Planetary Sciences, Raymond and Beverly Sackler Faculty of Exact Sciences, Tel Aviv University, Tel Aviv, Israel

Rotation of mid-latitude binary cyclones: a potential vorticity approach

B. Ziv[1] and **P. Alpert**[2]

With 14 Figures

Received March 11, 2002; revised June 27, 2003; accepted August 6, 2003
Published online November 20, 2003

Summary

Two cyclonic vortices close to each other, a 'binary cyclone' or 'binary system', tend to rotate cyclonically relative to one another and to merge, i.e. the "Fujiwhara effect". The point vortex model that represents barotropic binary cyclones predicts their rotation features as follows. The rotation rate is proportional linearly to the sum of the cyclones' intensities and inversely to the square of their separation distance while the more intense cyclone rotates slower. Our earlier observational analysis of 1423 mid-latitude binary cyclones (Ziv and Alpert, 1995) showed a reasonable fit to theory, except for the absence of a correlation between individual speeds and intensities within the binary systems, and a reversal of the inverse rotation-separation relationship at the range of 1400–1800 km.

This study is the first attempt to describe the mid-latitude binary systems using potential vorticity concepts (PV thinking), which implies that a binary interaction takes place between the 3-D flow patterns induced by upper-PV or surface-thermal anomalies rather than by the surface cyclones alone. It is argued that the upper-anomalies dominate the rotation process, and hence the rotational speeds of the interacting surface cyclones are more closely correlated with the relative intensities of their corresponding upper-level anomalies rather than with their own intensities, as reflected in weather charts. Data analysis indicates that mid-latitude binary cyclones are normally associated with at least one upper-PV anomaly. This explains the absence of a correlation between the rotation speed and the intensity of the surface cyclones there.

A unique type of a mid-latitude binary system is identified, in which one cyclone coincides with an upper major PV-anomaly and the other moves along the periphery of the former. Such a binary system is entitled here the 'Contact Binary System' (CBS), in contrast with remote interacting systems implied by the point vortex theory.

Analytical considerations yield an increase in the rotation rate with separation for CBSs of separation smaller than $\sim$1000–1500 km, in contrast to the normal decrease with R^2. The contribution of CBSs is suggested here to explain the abnormal increase in rotation rate at 1400–1900 km range.

1. Introduction

Two cyclonic vortices in close proximity, i.e. a binary cyclone, tend to rotate cyclonically relative to each other and to eventually merge (Fujiwhara, 1931). This interaction was entitled "the Fujiwhara effect" or "binary interaction". The rotational aspect of this interaction was quantitatively formulated for a barotropic fluid using the simple point vortex model (e.g. Lamb, 1945; Batchelor, 1980; Aref, 1983). According to this model each vortex, represented by an infinitely small core with positive vorticity, induces a circular flow pattern throughout the fluid. When applied to two cyclonic point vortices, denoted

1 and 2, with separation, R_{12}, the model yields the relative rotation rate ω,

$$\omega = \frac{k_1 + k_2}{R_{12}^2}, \tag{1}$$

Batchelor (1980), where k_1 and k_2 are their respective "intensities", i.e. the integrated relative vorticity over the cyclone's core. Their motions are directed perpendicular to their connection line and their respective individual speeds, V_1 and V_2, obey the ratio

$$\frac{V_2}{V_1} = \frac{k_1}{k_2}. \tag{2}$$

The binary rotation has, therefore, the following characteristics: (a) Cyclonic relative rotation with (b) a rate proportional linearly to the combined intensity and (c) inversely to the square of the separation distance while (d) the weaker cyclone rotates faster around the intense cyclone.

Several studies of the binary interaction (e.g. Haurwitz, 1951) has shown that for interacting cyclones with finite cores that do not overlap (remote interaction), Eqs. (1) and (2), hold. Therefore, they may be considered as valid for remote binary interactions in general, rather than only for two point vortices.

Extensive studies of binary tropical storms (e.g. Hoover, 1961; Brand, 1970; Dong and Neuman, 1983) have confirmed the existence of (a)–(c) in the tropical Pacific, but not in the tropical Atlantic. Brand (1970) found cyclonic rotation in the Pacific for cyclone pairs with separation distance smaller than 1300 km. The disagreement between theory and observations in the Atlantic was attributed to the effect of the background anticyclonic flow on the binary cyclones there (Dong and Neuman, 1983; Lander and Holland, 1993).

Extensive observational studies have indicated the existence of interactions that are far more complicated than the simple Fujiwhara effect, including rapid merging in some occasions and escape in others. The tropical binary interaction was also studied numerically. For example, Chang (1983) and DeMaria and Chen (1984), using a barotropic nondivergent model, showed a high sensitivity of the cyclones' tracks to the individual distribution of their tangential velocity. Richie and Holland (1993) and Holland and Dietachmayer (1993) studied the complexity of "non-Fujiwhara" effects through barotropic models, accounting for the role of the cyclones' fine structures and the convective cloudiness within them. Falkovich et al. (1995) examined the role of both beta effect and ocean feedback upon tropical binary storms. They found the beta effect to be a source of an asymmetry between the development of the intensities and tracks of the individual cyclones that take part in a binary interactions, whereas the ocean feedback has a dissipating effect on both this asymmetry and the system's intensity as a whole. Lester et al. (1998) classified the non-Fujiwara effects found among tropical cyclones in the north Atlantic and differentiated between internal factors, that are associated with an asymmetry between the interacting cyclones themselves, and external factors, that deflect the motion of one or both cyclones from that implied by the pure Fujiwara effect.

Ziv and Alpert 1995 (ZA95, hereafter) studied the rotational aspect of 1423 cyclone pairs that were found within the 30°–60° N, 0°–60° E domain for 24 winter months. An example of a cyclonic rotation is shown in Fig. 1. ZA95 found that when the separation distance between two cyclones is 2000 km or less, they rotate cyclonically on the average. They also found that in the subtropics (15°–30° N) the average rotation is anticyclonic, and attributed this to both the upper-level anticyclonic shear and to the prevalence of surface anticyclones there. In the mid-latitudes the background shear was found to have a significant enhancing effect only on cyclone pairs with separations smaller than 900 km. Renfrew et al. (1998) found binary rotation within pairs of Polar Cyclones with a good agreement with theory, especially when they reach their secondary (convective) stage.

The observed features of binary systems at the mid-latitudes found by ZA95 may be summarized as follows (also see Table 1).

- **Sense of rotation**: The rotation is cyclonic on the average up to 2000 km separation.
- **Intensity/rotation relationship**: The rotation rate increases with the sum of the intensities of the interacting cyclones.
- **Separation/rotation relationship**: The rotation rate decreases with separation distance

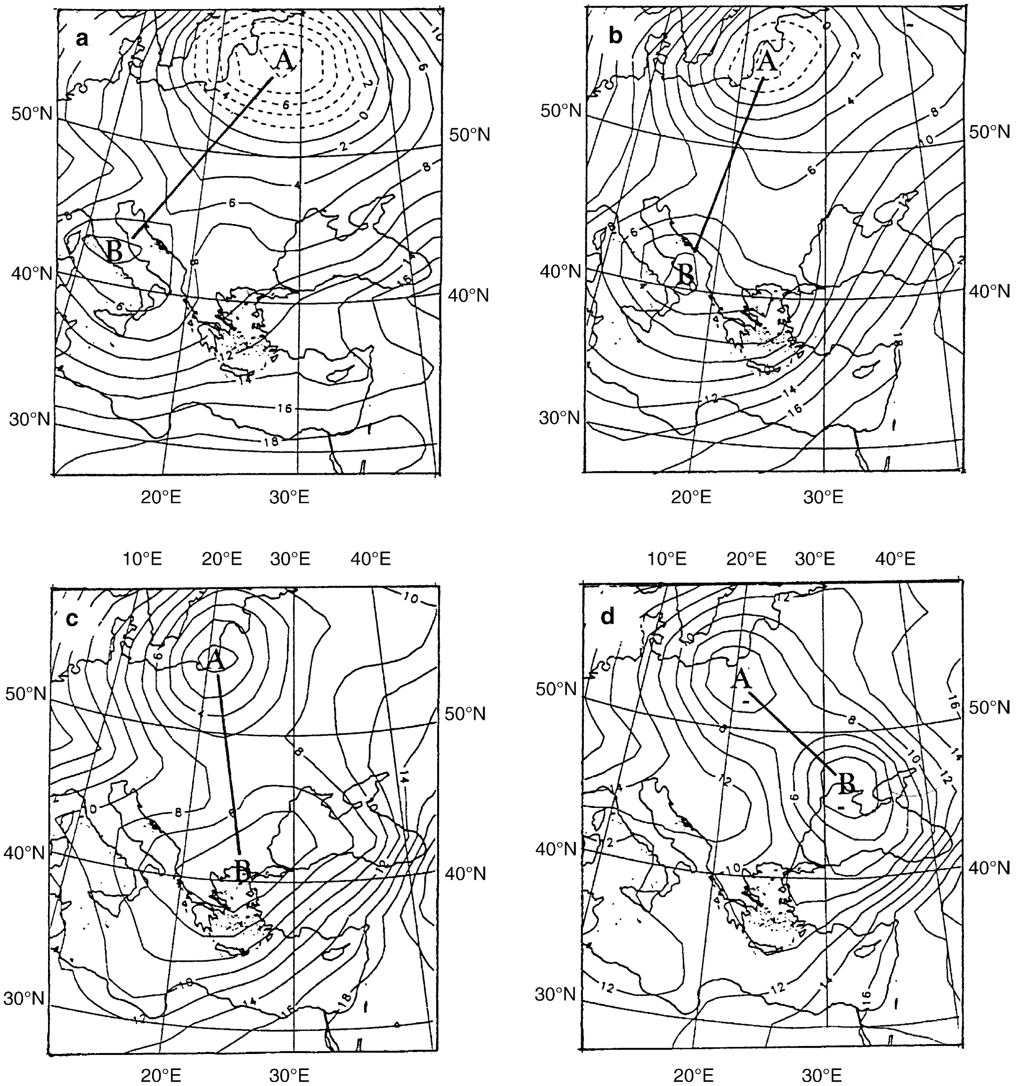

Fig. 1. 1000 hPa geopotential height distribution in dm with 1 dm interval for: (**a**) 00 UTC 22 Dec. 1986, (**b**) 12 UTC 22 Dec. 1986, (**c**) 00 UTC 23 Dec. 1986 and (**d**) 12 UTC 23 Dec. 1986. Cyclones composing the cyclone pair are denoted by A and B (following Ziv and Alpert, 1995)

Table 1. The characteristics of binary interaction according to the point vortex theory against that of the observed mid-latitude binary cyclones (following Ziv and Alpert, 1995)

Characteristic	Findings	Comments
Cyclonic rotation	up to 2000 km separation	observed values agree with theory
Rotation/separation relation	agreement up to 1400 km	unexplained peak near 1900 km
Rotation/intensity relation	agreement	"cyclone intensity" – its geopotential minimum
Speed-intensity relation	no significant relation	theoretical relation was found at 500 hPa level

up to about 1400 km, then the curve reverses its slope between 1400 and 1900 km with a pronounced peak near 1900 km (Fig. 2).

- **Intensity/rotational speeds ratio within the binary systems**: No significant correlation was found.

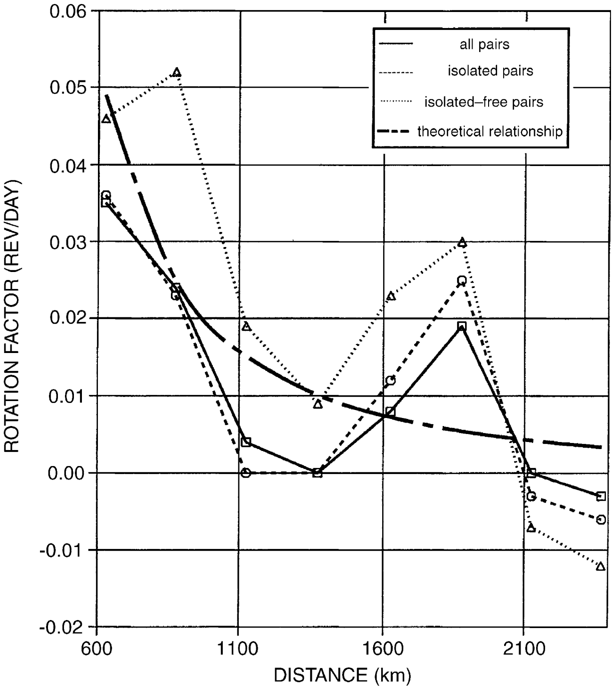

Fig. 2. Average rotation factor as a function of separation for the period 1982–1988, months December–March for the domain 30–60° N/0–60° E of all cyclone pairs (solid), 'isolated' pairs (dashed) and for 'isolated' and 'free' pairs (dotted). The semi-dashed line shows the 2-D theoretical relationship. 'Isolated' pairs are pairs around which no other cyclone was found within 1000 km radius, and 'free' pairs are pairs that any of its member was not located within a cyclogenetic area (following Ziv and Alpert, 1995)

The above findings agree with the point vortex model, except for two disagreements: one is the reversal of the predicted separation-rotation relation for separations of 1400–1900 km, second is the lack of correlation between rotation speeds and intensities within the binary systems.

ZA95 attributed these disagreements to the baroclinicity typifying the mid-latitudes, which does not exist in the 2-D point vortex model. Indeed, the disagreements nearly disappeared in a parallel analysis of the 500 hPa binary systems (ZA95), perhaps due to the more barotropic-like nature of the flow at this level, as compared to that on the surface.

Haurwitz (1951) stated that "it seems unlikely that the theory in its simple form can be applied generally to extratropical cyclones and anticyclones because the deviations from barotropic stratification are presumably large, so conditions aloft are quite different from those near the surfaces." This statement and the findings described above provided our motivation to extend the traditional approach beyond the 2-D framework in order to better describe qualitatively the mid-latitude binary interactions and to try explaining the disagreements between their observed features as compared with both that found in the tropics and that predicted by the 2-D model. We replace the 2-D vorticity by the 3-D counterpart, i.e. by the Ertel Isentropic Potential Vorticity (PV). The use of PV concepts is also called "PV thinking" (Hoskins et al., 1985; HMR hereafter). "PV thinking" considers a surface cyclone as a reflection of anomalies either in the upper-PV or in the surface-θ fields, implying that the use of a surface pressure chart for studying the binary interaction may yield misleading results.

The next section outlines the two basic types of cyclones according to "PV thinking" and discusses their implications to the binary interaction. Section 3 demonstrates the hypothesized features through the analysis of upper-PV and lower-θ fields in association with two mid-latitude binary episodes. Section 4 describes a distinct group of mid-latitude binary cyclones that we have identified and discusses its unique rotational features. The last section summarizes the results and their implications to the observed mid-latitude binary interactions.

2. Binary interaction as interpreted by "PV thinking"

The potential vorticity (PV) is given, under hydrostatic conditions, by

$$\mathrm{PV} = g\zeta \frac{\partial \theta}{\partial p}, \qquad (3)$$

(following Rossby, 1940 and Ertel, 1942), where p is pressure, g is gravity acceleration, ζ is the vertical component of the absolute vorticity, derived on isentropic surfaces, and θ is the potential temperature. PV and potential temperature are the only Lagrangian invariants of a 3-D adiabatic and frictionless flow (Egger, 1989). Large and synoptic-scale atmospheric systems can be assumed adiabatic and frictionless (Holton, 1992). For "balanced dynamical phenomena . . . the dynamical evolution can be described solely in terms of the PV (and surface potential temperature) distributions, their induced wind fields and their advective rates of change" (HMR). The "Invertibility Principle" states that "given the PV distribution, one can deduce the wind, pressure and temperature field" (HMR).

Inversions of PV and surface potential temperature fields show that a surface cyclone reflects a positive anomaly in the upper-level PV or in the surface potential temperature (Thorpe, 1985; HMR). Moreover, each of such a positive anomaly induces cyclonic flow over its surroundings. Hence, one may expect the detailed interaction among neighboring cyclones to depend on the structures of the 3-D flow patterns induced by their 'source anomalies'. In the following discussion, a cyclone associated with an upper-level PV anomaly will be referred to as a "cold cyclone" and that associated with a surface thermal anomaly as a "warm cyclone" though in real situations a cyclone may reflect a combination of both (e.g. a baroclinic cyclone, HMR). Figure 3 shows cross-sections through these two cyclone types following Thorpe (1985) as appears in HMR. They were derived by inverting the PV field for uniform conditions, with a positive circular symmetric near-tropopause PV anomaly (a) and a surface thermal anomaly (b), of 1667 km radius. Each type of anomaly induces a cyclonic tangential flow, attaining its maximum within its periphery and extending out of its boundaries, thus enabling a remote interaction with neighboring anomalies. The induced flow patterns of the two types differ substantially in their vertical distribution. The induced flow of the upper-PV anomaly maximizes at the tropopause and falls to about 60% of its maximum speed near the surface, while that induced by a surface thermal anomaly maximizes at the surface, but falls sharply with height, reaching only about 20% of its maximum value at the tropopause level.

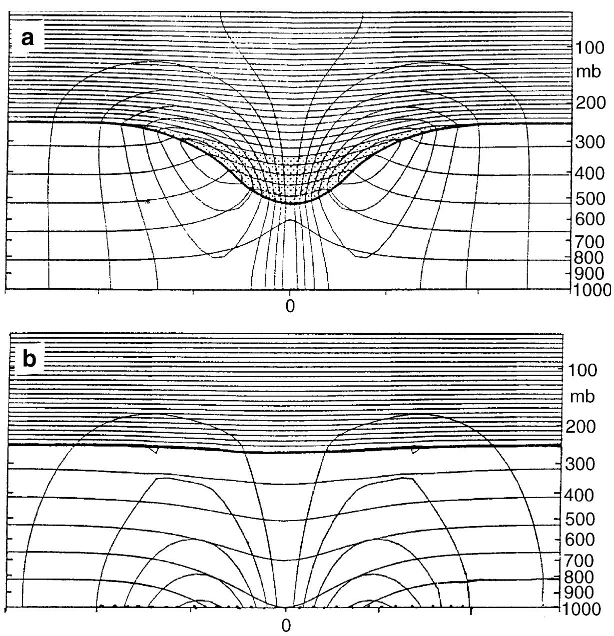

Fig. 3. Cross-sections through circular symmetric circulations induced by isolated positive anomalies (whose location is shown stippled) **a** in near-tropopause PV and **b** surface potential temperature anomalies produced by HMR. Thin lines represent both isentropes and tangential velocity. Bold lines indicate the tropopause

Of course, the vertical penetration of the induced flow depends on the horizontal scale of the pertinent anomaly, but in the context of binary interactions it can be concluded that upper-PV anomalies tend to drive a surface-thermal anomaly, and their associated warm cyclone, faster than in the opposite direction, i.e. that lower-thermal anomalies would drive upper-PV anomalies. Hence, the upper anomalies, when they exist, dominate the binary interactions.

The nature of the inversion operator (HMR) implies that both the speed of the induced flow and the intensity of the surface cyclone would be proportional to the intensity of its source anomaly. Therefore, the advective power of each of the interacting surface cyclones may, to a first approximation, be proportional to its intensity, as implied by the 2-D approach. This may be a rather realistic assumption for a system consisting of two warm cyclones, since the source anomalies and their associated cyclones are at the same level. But, for cold cyclones this is not generally true, since the intensity of a surface cyclone is also affected by the lower-level thermal field. Moreover, upper-troposphere positive PV anomalies often tend to coincide with lower-cold anomalies (HMR; Alpert, 1984) which reduce the intensity of the surface cyclones associated with the former. Hence, in binary systems associated with at least one upper-PV anomaly, the correlation between the ratios of the rotation speeds and the intensities of the surface cyclones is expected to be poor. The above can be generalized by saying that when two upper-PV anomalies are involved in a binary interaction, the rotation rate of their associated cyclones would obey Eqs. (1) and (2), but with respect to the intensity of the upper-anomalies rather than with that of the surface cyclones.

The PV approach shifts our attention from the surface cyclones toward the source anomalies as the interacting objects, so the concept "binary system" would be preferred over "binary cyclone" for the mid-latitudes. The main implication of this approach is that whenever upper-PV anomalies exist in a binary system, they dominate the rotation of the system.

3. Analysis of the observed binary systems

The observational study is based on ten cases of binary interaction that lasted for at least 36 hours, in which the binary system completed rotation of 70° or more. For each case a time series of surface pressure charts presents the rotation process, the lower-level thermal field and the upper-level PV-field, show the structure and rotation of the respective source anomalies. Two cases are presented below. They represent two different types of binary systems: in the first, one of the two interacting cyclones is cold while the other is baroclinic, i.e. associated with the two types of source anomalies at different locations. In the second case, one of the interacting cyclones is cold and the other – warm. No case of pure warm binary system was found north of 30° N.

The analysis makes use of ECMWF initialized data (Bengtsson et al., 1982; Haseler and Sakellarides, 1986; Hollingsworth et al., 1986) containing three wind components, geopotential height and temperature on seven mandatory pressure levels for the area 0°–60° N, 0°–60° E. For each case, three fields are shown: First, the 1000 hPa geopotential height, representing the surface pressure; second the 850 hPa potential temperature, representing the surface thermal field; and third, the PV on the isentropic level which represents, more or less, the tropopause for the relevant case. The 850 hPa surface was chosen for representing the "surface" thermal field in order to avoid the small scale features and the diurnal effects within the planetary boundary layer (HMR). The isentropic PV field was extracted from the isobaric data, assuming linear dependence of temperature on the log-pressure between successive pressure levels, which was found by Ziv and Alpert (1994) to be superior to other interpolation methods.

The cases presented below were extracted by the analysis system developed by Neeman and Alpert (1990). The surface interacting cyclones, i.e. the 1000 hPa geopotential minima, are denoted "A" and "B", and the increments of their motions within the ensuing 36 hours, at 12 h intervals, are depicted. Several approaches for identifying an 'anomaly' may be used. This subject is discussed in Appendix A. Here, a local maximum or a pronounced "tongue" in the thermal/PV field is considered as an anomaly. A notation "A" or "B" refers to the source anomaly of the respective surface cyclone. For each case the relative rotational speeds of the interacting surface cyclones are compared with their individual intensities, then with that of their associated PV anomalies. Due to the illustrative nature of this part of the study the intensities are evaluated qualitatively.

3.1 Case 1: 3–4 January 1985, cold-baroclinic binary interaction

Figure 4 shows two cyclones, denoted A and B, located initially, in 00 UTC 3 January 1985, in

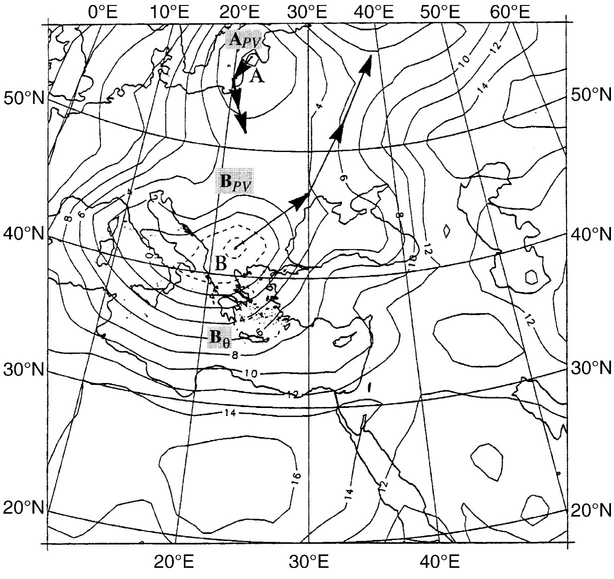

Fig. 4. 1000 hPa geopotential height distribution in dm, with 1 dm interval, for 00 UTC 3 Jan. 1985. Cyclones composing the pair are denoted by A and B. The location of the source PV anomaly of cyclone A and the source PV and θ anomalies of cyclone B are denoted A_{PV}, B_{PV} and B_θ, respectively. The arrows represent their movements for 3 time increments of 12 h

Lithuania (57° N, 22° E) and in the Balkans (42° N, 23° E), respectively, subjected to a cyclonic rotation. The imaginary line that joins them rotated about 120° during 36 hours with only a slight decrease in length (R), about 1500 km. Cyclone B, however, moved much faster than cyclone A, though it was the deeper one, as reflected from the minimum in geopotential height. It may be argued that since both cyclones were steered by the mid-latitude upper-level westerlies, the relative westward progression of cyclone A was reduced and the eastward progression of cyclone B was enhanced. However, the meridional displacement of cyclone A was also smaller, about 4° latitudes, compared to 15° for cyclone B, suggesting that the latter indeed had a larger rotation speed. Figure 5 shows the 320 K isentropic PV field for 00 UTC 4 January 1985. Two positive PV-anomalies coincide more or less with the cyclones' locations. Anomaly A appears in Fig. 5 as a pronounced tongue that extended from the north and disintegrated 12 hours later, and B was a local maximum. They rotated in the same fashion as the surface cyclones. The central PV value of anomaly A was larger than that of anomaly B by over 0.5 PVU, implying that anomaly A was the more intense. Figure 6 shows

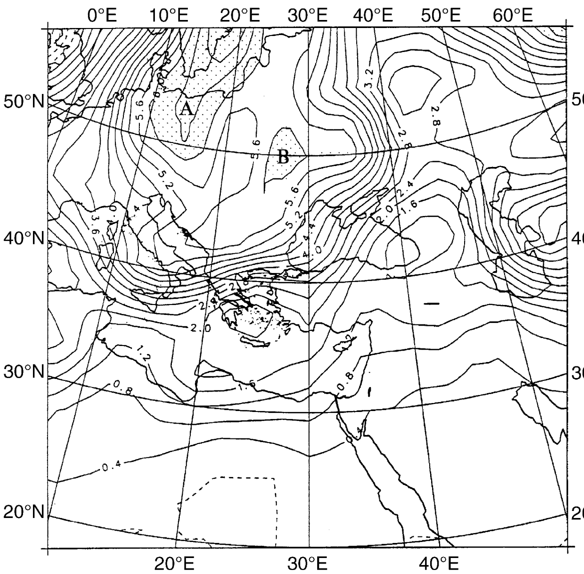

Fig. 5. Isentropic 320 K PV distribution in 1 PVU (PVU $= 10^{-6}\,m^2\,s^{-1}\,K\,kg^{-1}$), with 0.4 PVU interval, for 00 UTC 4 Jan. 1985. Areas with values exceeding 6 PVU are shaded. The positive anomalies corresponding to cyclones A, B are denoted, respectively

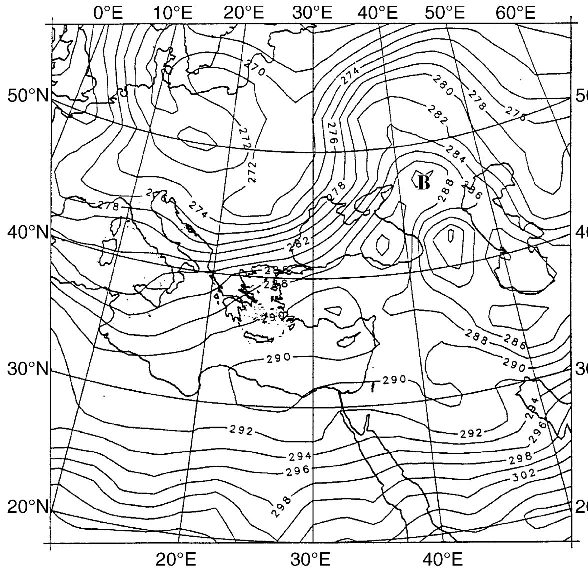

Fig. 6. 850 hPa potential temperature distribution for the same time as in Fig. 5. The anomaly associated with cyclone *B* is denoted

the 850 hPa θ field for 00 UTC 4 January 1985. No thermal anomaly is found in the vicinity of cyclone A, but a maximum was found north of the Black Sea (48° N, 42° E), about 6° to the south east of the cyclone B. This anomaly, denoted B_θ in Fig. 4, progressed toward the north–east, maintaining its location relative to the cyclone. The thermal anomaly B_θ may explain why the location of cyclone B did not coincide with the upper PV anomaly B, but to the east, between the two source anomalies. The combined contributions of both anomalies explain also why cyclone B was deeper than cyclone A by 40 m (Fig. 4). However, the rotation speed of cyclone B does not seem to be related to its intensity relative to cyclone A, but rather to that of its source upper anomaly.

3.2 Case 2: 10–11 January 1984, cold-warm binary interaction

Figure 7 shows a cyclone pair, denoted A and B, located over south Italy (41° N, 15° E) and Tunis (36° N, 8° E), respectively, undergoing a cyclonic rotation. Cyclone A remained nearly stationary (except for a slight southward movement) while cyclone B revolved around it counterclockwise by about 80° within 36 hours. This seems to contradict the observed similarity between the

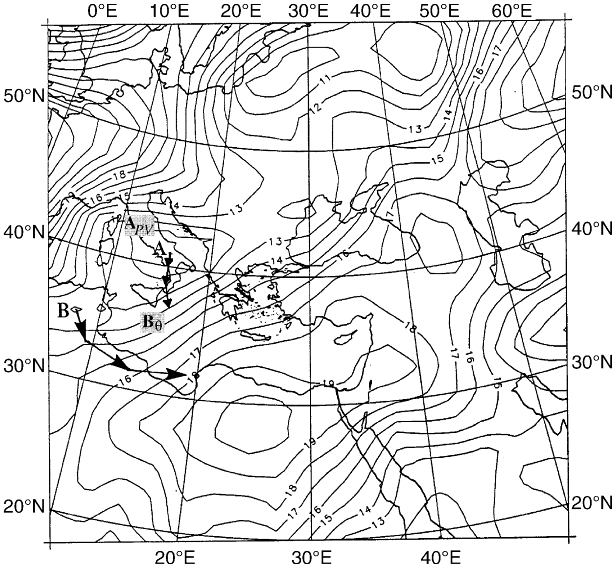

Fig. 7. 1000 hPa geopotential height distribution in dm, with 1 dm interval, for 00 UTC 10 Jan. 1984. Cyclones composing the pair are denoted by A and B. The locations of their source anomalies are denoted A_{PV} and B_θ. The arrows represent their movements for 3 time increments of 12 h

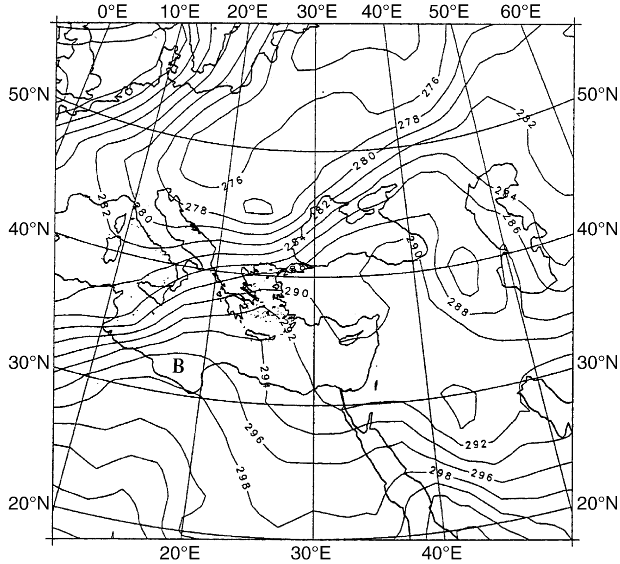

Fig. 9. 850 hPa potential temperature distribution for the same time as in Fig. 8. The anomaly associated with cyclone *B* is denoted

intensities of the two cyclones for the major part of the period, i.e., their geopotential heights differed by only 20 m. The upper PV and the lower thermal fields, however (Figs. 8 and 9 respectively), indicate that cyclone A coincided with a PV maximum centered over central Italy, whereas cyclone B was associated with a thermal anomaly extending from northern Africa to the middle Mediterranean and later moved eastward. The asymmetry between the types of their source anomalies is suggested here to explain why cyclone B dominated the rotation.

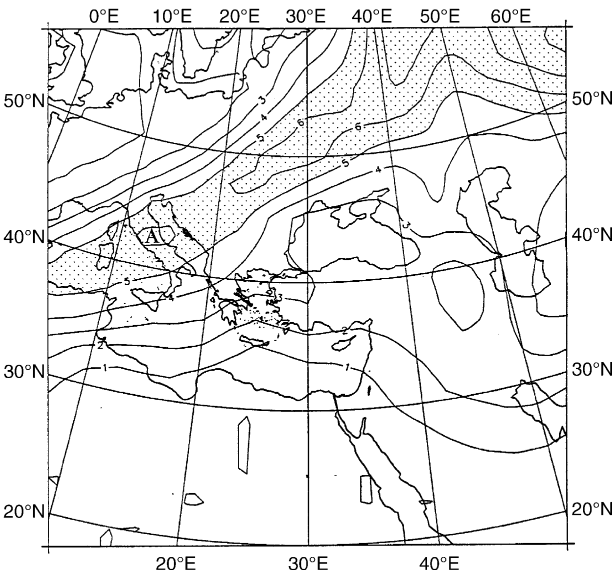

Fig. 8. Isentropic 330 K PV distribution in 1 PVU, with 1 PVU interval, for 00 UTC 11 Jan. 1984. Areas with values exceeding 3 PVU are shaded. The positive anomaly corresponding to cyclone A is denoted

These two cases are in line with the hypothesized features of the binary rotation described in Sec. 2. One feature is that in an interaction in which two upper-PV anomalies are involved, the cyclone that is associated with the more intense anomaly moves slower. The second is that in a warm-cold interaction, the warm cyclone revolves around the cold one and does not follow the ratio of the intensities of the surface cyclones, i.e. Eq. (2). A further analysis of the above cases, as well as other eight cases (not shown), has yielded a refined description of a unique type of mid-latitude binary system, as described in the following section.

4. The contact binary system (CBS)

So far the binary systems were considered as remotely interacting. This implies that each of the two individual anomalies involved in a binary interaction is assumed to be small as compared with the separation distance between them. The data analysis of the mid-latitude binary systems, however, have indicated that in quite a number of cases one of the interacting anomalies is relatively large, so that the other is located at its periphery. This has led us to propose the term "contact binary interaction" for such a case, and the name "Contact Binary System" (CBS) for the pertinent system. The CBSs were found to have common unique features. This section outlines these features. First the unique structure of a CBS is described, then its rotational characteristics are derived. The last subsection discusses the impact of their existence on the observed abnormal increase in the rotation rate with separation distance of mid-latitude binary systems in the 1400–1900 km range found by ZA95.

4.1 Structure

The main features of a CBS are shown schematically in Fig. 10. One of the cyclones, L_1, is associated with a major upper PV anomaly, often associated with closed PV-contours. The other cyclone, L_2, is associated with a thermal anomaly, sometimes combined with an upper-PV secondary anomaly, at the periphery of the primary one, to its south–east (e.g. case 2 above). The CBSs may explain the higher observed frequency of binary cyclones oriented in a northwest–southeast direction (Fig. 11). Cyclone L_1 will be referred to as the primary cyclone, and cyclone L_2 as the secondary one.

In cases where the secondary cyclone reflects combined contributions of two anomalies,

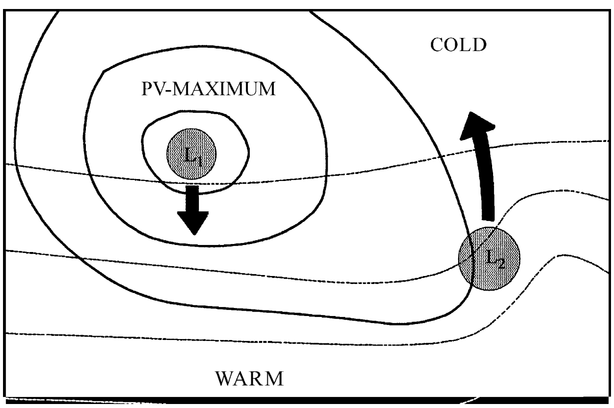

Fig. 10. A schematic picture of a typical mid-latitude Contact Binary System (CBS). Solid lines are upper-level PV isolines and dotted-thin lines are surface isotherms. The surface cyclones, denoted L_1 and L_2, are represented by dotted circles and their velocities by thick arrows

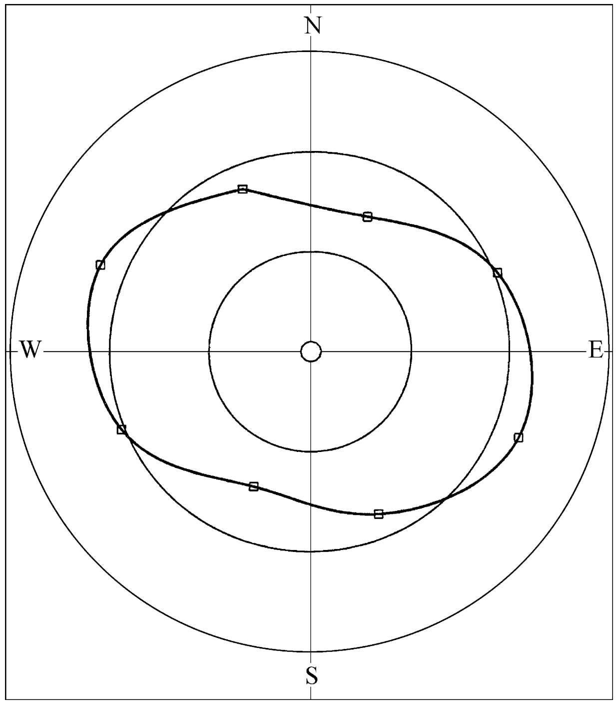

Fig. 11. Polar diagram showing the distribution of the orientations of mid-latitude binary cyclones that were observed (ZA95). This is based on the subset of 327 cyclone pairs, each of which had a separation less than 2100 km, free from any additional cyclone within 1000 km distance and located out of cyclogenetic areas (ZA95). Distance from the center is proportional to the number of occurrences. Each sector is of 45° and is represented by its central point. The 270°–315° (90°–135°) sector, for instance, is the most frequent with 15% of the occurrences

cyclone L_2 may be more pronounced than cyclone L_1 at the surface. But, since it is associated with the weaker upper-PV anomaly, cyclone L_2 rotates faster than L_1. In this way, the CBSs contribute to the discrepancy in the intensity/rotation relationship for the surface binary systems as found by ZA95. Moreover, the typical location of the primary cyclone L_1 to the north of the secondary cyclone L_2 (Fig. 10) implies that L_1 is expected to move to the west, but this movement is suppressed by the steering effect of the upper-level westerlies, resulting in its stationary appearance (Sec. 3).

The tendency for the secondary anomaly (L_2) to be formed and to move along the periphery of the primary cyclone (L_1) may be understood, following HMR. The primary L_1 positive PV anomaly, resulting from an equatorward displacement of a polar air mass, possesses low temperatures and high PV. Consequently, the boundaries of the

L_1 anomaly are highly baroclinic. This baroclinicity maximizes along the southern boundaries, so this sector becomes favorable for the formation and maintenance of disturbances, such as the L_2-type cyclones. The latter are, indeed, frequently found at the frontal zone, at the south–east sector of a Mid-latitude 'parent' cyclone. The Sharav Cyclones that tend to form in the spring season along the North African coast (Egger et al., 1994; Alpert and Ziv, 1989) are examples for such a system.

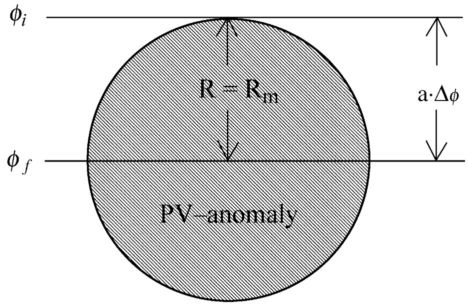

Fig. 12. Scheme of a circular upper-level PV anomaly (shaded) with radius R. The center originated from the latitude ϕ_i and has moved to the latitude ϕ_f

4.2 Rotation/separation relationship

Next, a relationship between the rotation rates of the CBSs and their separations is derived. The derivation is based on the following assumptions:

- The primary anomaly is assumed to be the result of an equatorward extension of an upper-level trough that turns into a cutoff cyclone (e.g. Palmen and Newton, 1969).
- The secondary anomaly is significantly smaller, both in size and in relative vorticity, compared to the primary one so
- The rotation of the CBS as a whole is determined by its motion around the primary (Fig. 10), and
- The velocity of the secondary cyclone is approximated by the tangential wind along the periphery of the primary anomaly.
- The wind and relative vorticity within the primary anomaly have both circular symmetry.

Consider a polar air mass with zero relative vorticity that is centered at a polar latitude ϕ_i. The air mass possesses an absolute vorticity $f(\phi_i)$, larger than those characterizing the mid-latitudes, and is displaced equatorward to a mid-latitude ϕ_f (Fig. 12). Conservation of absolute vorticity implies that when migrating, the air-mass would acquire positive relative vorticity (ζ) with a central value of $\zeta_{\max}$, which is opposite and equal in magnitude to the respective change in the Coriolis parameter, Δf, i.e.

$$\zeta_{\max} = -\Delta f = f(\phi_i) - f(\phi_f). \tag{4}$$

Based on the beta-plain approximation,

$$\Delta f = \beta \cdot \Delta y, \tag{5}$$

where Δy is the meridional displacement of the air mass and $\beta \equiv \frac{\partial f}{\partial y} \cong \frac{2\Omega \cos(\varphi_0)}{a}$. Substituting 45° for φ_f and assuming that Δy is equal to the radius R_m of the air mass (Fig. 12) yield

$$\zeta_{\max} \cong \frac{\sqrt{2}\Omega}{a} R_m. \tag{6}$$

If the meridional gradient in vertical stratification is not accounted for, Eq. (3) implies that the amplitude of the PV anomaly would be equal to $\zeta_{\max}$.

Actually, the air mass would adjust itself so that the PV would be partitioned between vertical stratification and absolute vorticity according to its horizontal scale. Under quasi-geostrophic conditions the vorticity anomaly can be deduced from an anomaly in the stream function, ψ, given by

$$\psi = \psi_0 e^{-r/R} e^{-f(z-z_0)/NH}, \tag{7}$$

where r and z are horizontal and vertical coordinates, R, H are the horizontal and vertical scales, respectively, N is the Brunt-Vaisala frequency and z_0 is the height of the anomaly. Following HMR, the vorticity anomaly, ζ, and vertical stratification anomaly, s, are obtained from the second derivatives in r and z, respectively, i.e.

$$\zeta = \frac{1}{R^2}\psi; \quad s = \frac{f^2}{N^2H^2}\psi. \tag{8}$$

The approximate ratio between the vorticity at the anomaly center, ζ_0, and the maximum PV anomaly, $\zeta_{\max}$, is, therefore,

$$\frac{\zeta_0}{\zeta_{\max}} \cong \frac{1}{1 + \frac{f^2R^2}{N^2H^2}} \tag{9}$$

The same relation is obtained when a Gausian distribution of ψ is applied in (7). Inserting (9) in (6) yields

$$\zeta_0 \cong \frac{\sqrt{2}\Omega}{a}\left(\frac{R_m}{1+\frac{f^2R_m^2}{N^2H^2}}\right) \tag{10}$$

The tangential speed along the periphery, V, may be obtained from the circulation, C, which is given, following the Gauss theorem, by integrating the vorticity over the anomaly's core, i.e.

$$C = 2\pi\int_0^{R_m}\zeta r\,dr = 2\pi\int_0^{R_m}\zeta_0\,\mathrm{F}\left(\frac{r}{R_m}\right)r\,dr$$
$$= 2\pi\zeta_0\chi R_m^2, \tag{11}$$

where $\mathrm{F}(r/R_m)$ is a dimensionless circularly symmetric vorticity distribution and

$$\chi \equiv \int_0^{R_m}\mathrm{F}\left(\frac{r}{R_m}\right)r\,dr, \tag{12}$$

The tangential wind speed is, then,

$$V = \frac{C}{2\pi R_m} = \zeta_0\chi R_m, \tag{13}$$

and the rotation rate ω is

$$\omega \cong \chi\frac{V}{R_m} = \chi\zeta_0$$
$$= \chi\frac{\sqrt{2}\Omega}{a}\left(\frac{R_m}{1+\frac{f^2R_m^2}{N^2H^2}}\right). \tag{14}$$

Assuming that the vorticity distribution within the anomaly, and hence χ, are independent on the anomaly size, the dependence of ζ_0 on R_m for various CBSs, determines the ω-R relationship. The rotation attains its maximum at

$$R_m = \frac{NH}{f}. \tag{15}$$

A substitution of 10^{-2}, 10^4 and 10^{-4} for N, H and f, respectively, in (15) indicates that the maximum rotation rate would be found around a 1000–1500 km separation distance. The existence of CBSs explains the observed increase in the rotation-separation relationship found between 1400 and 1900 km separation (Fig. 13).

4.3 Quantitative estimate of the rotation rate

In order to evaluate the expected rotation rates for CBSs the dimensionless vorticity distribution

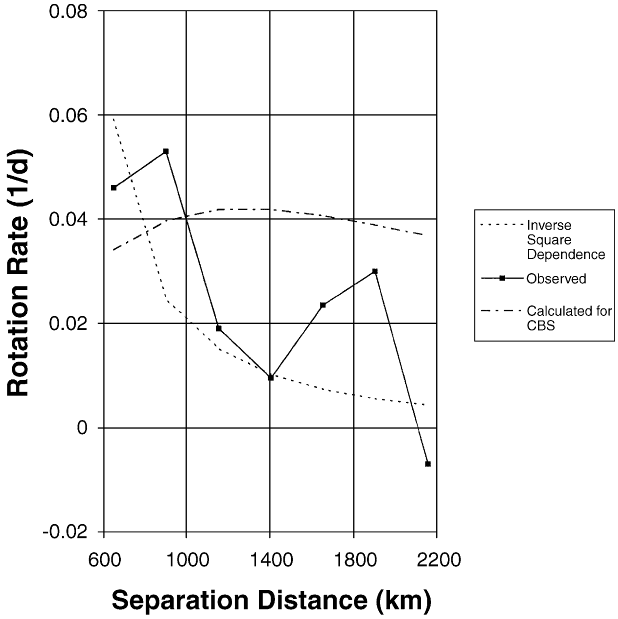

Fig. 13. Variation of average rotation factor for cyclone pairs as a function of separation for isolated-free pairs (Fig. 2). Dashed line represents the theoretical point vortex relation (Eq. (1)) and the semi-dashed line – the relation for the CBS proposed here (Eq. (14)) with $\chi = 0.3$

χ and the scaling factors, H and N, must be specified. It is worth noting that χ has a key role in the detailed binary interaction in the tropics (Chang, 1983; DeMaria and Chen, 1984). Two vortex types are most common in the literature. One is the "patch vortex", or the "Rankine vortex", in which the relative vorticity is uniform all over its core. This type was adopted by Haurwitz (1951) for the tropical storms, but seems to be less appropriate for mid-latitude cyclones, where a pronounced decrease in vorticity with distance from the vortex center is found (not shown). Another type is the "cosine vortex", for which $F(r/R_m) = 0.5[\cos(\pi r/R_m) + 1]$. This type was applied by Thorpe (1985) for temperature departures from normal within the PV and θ anomalies. The values of χ are 0.5 for the Patch vortex and 0.15 for the Cosine vortex. The actual PV distributions within positive anomalies (see Figs. 5, 8) seem to have distributions which are between the uniform and cosine distributions, so $\chi = 0.3$ was adopted. The values applied for H and N are 8×10^3 m and 10^{-2} s^{-1}, respectively.

Figure 13 shows 3 curves of rotation rate as a function of separation, i.e., the observed for isolated-free pairs (Fig. 2), the theoretical point vortex relationship (Eq. (1)) and the relation corresponding to the CBS proposed here (Eq. (14)). The observed curve follows, more or less, the point vortex curve for small separations up to 1400 km, then changes its slope abruptly and approaches the values corresponding to that of the CBS near 1900 km separation and finally drops sharply and intersects the zero line at about 2100 km. The sharp increase in the observed R-ω relation can be attributed to an increase in the proportion of CBSs to the total binary systems, suggesting that larger upper-level cutoff cyclones are more favorable for formation of secondary disturbances, and hence for CBSs. Moreover, the 1400 km distance seems to be a lower limit for CBS formation. The sharp decrease of the R-ω relation for separations around 2000 km may be interpreted as the combined result of an upper limit of the upper-level cutoff cyclones' radius and the approach to the influence range of binary interaction, being 2000 km (ZA95).

5. Summary and discussion

This study is the first attempt to describe the binary interaction from a PV viewpoint. This approach is adopted here for the mid-latitude binary cyclones, and is used to study their rotational features. "PV thinking" refers to surface cyclones as the projections of upper-PV or lower-θ positive anomalies or some combination of both. The traditional 2-D approach is extended here to the 3-D domain, enabling the inclusion of baroclinicity, which characterizes the mid-latitudes. Our study differs from the traditional point vortex approach in two aspects:

- The PV and thermal *anomalies* are considered as the interacting objects rather than the *surface cyclones* alone.
- The *contact interaction* is introduced and, along with the *remote interaction*, is shown to provide a more comprehensive picture of our earlier findings.

The study has two objectives: one is to better describe the structure and behavior of the mid-latitude binary systems. Second, is to explain the disagreements between the observed rotational features of the mid-latitude binary cyclones (ZA95) and the predictions of the point vortex model, which agrees with the observed rotation of tropical binary cyclones.

The PV concepts, when applied to binary systems, lead to the following conclusions:

- Whenever significant upper-PV anomalies are involved, they dominate the rotation process.
- Consequently, the individual rotation speed of each surface cyclone is proportional to the intensity of the source *upper-anomaly* of the other cyclone rather than with its own intensity.

The latter explains the lack of correlation between the intensities of the surface cyclones and their rotation speeds within mid-latitude binary systems, found by ZA95, as predicted by the point vortex model. These conclusions are illustrated by case studies, two examples of which are shown in Sec. 3 above.

A further examination of data has indicated the existence of a distinct type of mid-latitude binary system. This type is entitled here "Contact Binary System" (CBS). The CBS is composed of one cyclone that is associated with a major upper-PV anomaly and another, located at its southeast periphery, normally associated with a lower-thermal anomaly, sometimes combined with a secondary upper-PV disturbance. Analytical considerations indicate that for CBSs the rotation rate has a unique dependence on separation distance, with a maximum near 1300 km separation.

Data analysis, when interpreted through PV thinking, yields the following conclusions:

- A mid-latitude binary system is associated with at least one upper-PV anomaly.
- The dominance of the upper-PV anomalies over the rotation process implies that the individual rotational speeds of the interacting cyclones are better correlated with the relative intensities of the upper-level anomalies than with those of the surface cyclones. This hypothesis agrees with the analysis of binary interactions at the 500 hPa level, ZA95.
- The population of mid-latitude binary systems is partitioned between remotely interacting and contact interacting systems (CBSs).
- CBSs are suggested here as the contributors to the observed increase in separation/rotation relationship for 1400 to 1900 km separation distances, ZA95, and a theoretical basis for this increase is derived.

"PV thinking" probably explains also the difference between the maximum distance where binary interaction dominates in the mid-latitudes (2000 km, ZA95) and in the tropics (1300 km; Brand, 1970). Since the binary interaction in the mid-latitudes is dominated by cold cyclones while that in the tropics – by warm cyclones, this difference may represent a respective difference in their radii of influence. The wind patterns that were derived for the two cyclone types (HMR, Fig. 3) differ, indeed, in their horizontal distribution. The surface wind at the lateral boundaries of the domain is about 20% of its maximum value for the former, but only to about 10% for the latter, though the horizontal radii of the two source anomalies are the same.

An interaction between more than two neighboring cyclones may sometimes occur, with increased complexity in the motion of individual cyclones (Aref, 1983). A relatively simple example is the interaction between the intense polar vortex and the mid-latitude cyclones. This vortex, with its large vertical scale and horizontal dimensions, and its induced mid-latitude westerlies, drives the relatively weaker mid-latitude anomalies, and their associated surface cyclones, to revolve around it. At the same time, mutual interactions among these relatively weak anomalies are superposed upon the major interaction.

The differentiation between binary rotation and the steering by the ambient flow is not elaborated here. If both anomalies were advected by the same flow, this effect could be eliminated by simply evaluating the rotation of the vector connecting the two rotating cyclones, as is done here. But, if each anomaly is steered by a different ambient flow (as is the case for surface-upper system) the contribution of the differential advection may complicate the situation. Assuming that the ambient flow is zonal, this effect can affect the relative motions of the rotating cyclones when the cyclones are located at different latitudes. This is relevant to case 2 (Fig. 7), when the upper-level flow is expected to drive anomaly (A) eastward and the surface flow is expected to drive anomaly (B) westward, implying a negative contribution to the relative rotation of the cyclone pair. The significant positive rotation observed suggests that the effect of the mean flow is secondary with respect to that of the mutual interaction (ZA95).

The PV approach, when used for describing mid-latitude binary cyclones qualitatively, is found here capable of describing the mid-latitude binary interactions and to explain the discrepancies between the barotropic theory and observed characteristics. This work can serve as a preliminary conceptual basis for future quantitative study, based on inversion of PV fields.

Appendix A: identification of anomalies

The concept of 'anomaly' refers to a local or regional deviation of a field from a reference value. The amplitudes and geometrical shapes of the anomalies depend on the choice of the reference state. Some examples follows.

(*a*) *A uniform reference state*. HMR use anomalies (Fig. 3) relative to a uniform reference state. Therefore, the PV field at a certain isentropic level is displayed after the subtraction of a constant value. This approach preserves the original distribution regardless of the chosen reference state's value.

(*b*) *A zonal reference state*. A PV or θ anomaly may also be defined relative to a nonuniform, e.g. zonal, reference state. An anomaly may thus change its amplitude as it migrates meridionally, since only its absolute value is to be conserved. The choice of a zonal reference state may be made in several ways. One is to multiply the local Coriolis parameter by the zonal average stability parameter, ignoring the large-scale circulations (HMR). Other may be obtained by averaging the PV over the latitudinal belt or by multiplication of the average absolute vorticity

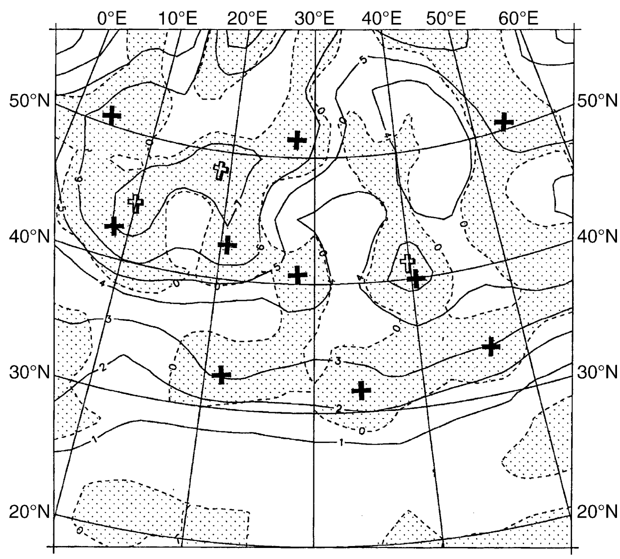

Fig. 14. Isentropic 360 K PV-distribution for 00 UTC Jan. 3 1985 in PVU with an interval of 1 PVU (solid). The areas where the Laplacian of the PV is negative, indicating positively anomalous PV, are shaded. Three PV maxima are found north of 30° N, whereas the Laplacian has at least 10 maxima in addition to those which coincide with the PV maxima

by the average stability parameter. These approaches are not identical. Due to the inherent ambiguity of these approaches, they were not adopted.

(*c*) *Mapping the Laplacian of the PV.* Mapping the Laplacian of any field enhances local deviations in the relevant variable, i.e., anomalies. However, this operator is very sensitive to small-scale features, what makes it hard to visualize the synoptic scale systems, see e.g. Fig. 14. HMR stress that PV charts magnify the synoptic-scale systems, because of the laplacian-like nature of the relative vorticity field with respect to the geopotential height field.

For the above argument a local maximum or a pronounced "tongue" of positive PV or potential temperature is referred to as an anomaly in this study.

Acknowledgments

We thank the German Israeli Foundation (GIF) I-138-120.8/89 for supporting this research. Thanks to ECMWF for the data, to Prof. B. Hoskins and Prof. J. Egger, who reviewed this paper, and to Prof. M. McIntyre, Prof. A. Thorpe, Dr. E. Heifetz and Dr. A. Tafferner for valuable discussions. Thanks to support from the EU project DETECT and to the GLOWA-JR project funded by BMBF and MOS.

References

Alpert P (1984) An early winter subtropical cyclone in the eastern Mediterranean. Isr J Earth Sci 33: 150–156

Alpert P, Ziv B (1989) The Sharav Cyclone: observations and some theoretical considerations. J Geophys Res 94: 18,495–18,514

Aref H (1983) Vortex motion. Ann Rev Fluid Mech 11: 95–122

Batchelor GK (1980) An introduction to fluid dynamics. Cambridge: Cambridge University Press, 615 pp

Bengtsson L, Kanamitsu M, Kallberg P, Uppala S (1982) FGGE 4 – dimensional data assimilation at ECMWF. Bull Amer Meteor Soc 63: 29–43

Brand S (1970) Interaction of binary tropical cyclones of the western North Pacific Ocean. J Appl Meteor 9: 433–441

Chang SW (1983) A numerical study of the interaction between two tropical cyclones. Mon Wea Rev 111: 1806–1817

DeMaria M, Chan JCL (1984) Comments on "A numerical study of the interaction between two tropical cyclones". Mon Wea Rev 112: 1643–1646

Dong K, Neuman CJ (1983) On the relative motion of binary tropical cyclones. Mon Wea Rev 111: 945–953

Egger J (1989) A note on the complete sets of material conservation laws. J Fluid Mech 204: 543–548

Egger J, Alpert P, Tafferner A, Ziv B (1994) Numerical experiments on the genesis of Sharav Cyclones: idealized simulation. Tellus 47A: 162–174

Ertel H (1942) Ein neuer hydrodynamischer virbelsatz. Met Z 59: 271–281

Fujiwhara S (1931) Short note on the behavior of two vortices, 3rd edn. Proc Physico-Mathematical Soc Japan 13: 106–110

Falkovich AI, Khain AP, Ginis I (1995) Motion and evolution of binary tropical cyclones in a coupled atmosphere-ocean numerical model. Mon Wea Rev 26: 1345–1363

Gill AE (1982) Atmosphere-ocean dynamics. NY: Academic Press, 662 pp

Haseler J, Sakellarides G (1986) Description of the ECMWF Model post processing system, Tech. Memo No. 121, ECMWF

Haurwitz B (1951) The motion of binary cyclones. Arch Meteor Geophys Biokl B4: 73–86

Holland GJ, Dietachmayer GS (1993) On the interaction of tropical-cyclone scale vortices. III: Continuous barotropic vortices. Quart J Roy Meteor Soc 119: 1381–1398

Holton JR (1992) An introduction to dynamic meteorology, 3rd edn. NY: Academic Press, 511 pp

Hoover EW (1961) The motion of hurrican pairs. Mon Wea Rev 89: 251–255

Hoskins B, McIntyre ME, Robertson AW (1985) On the use and significance of isentropic potential vorticity maps. Quart J Roy Meteor Soc 111: 877–946

Lamb H (1945) Hydrodynamics, 6th edn. NY: Dover Publication, 738 pp

Lander M, Holland GJ (1993) On the interaction of tropical-cyclone scale vortices. I: Observations. Quart J Roy Meteor Soc 119: 1347–1361

Lester E, Carr I, Mark Boothe A, Elsberry RL (1998) Observational evidence for alternate modes of track-altering binary tropical cyclone scenarios. Mon Wea Rev 125(9): 2094–2111

Neeman BU, Alpert P (1990) Visualizing atmospheric fields on a personal computer: Application of potential vorticity analysis. Bull Amer Meteor Soc 71: 154–160

Palmen E, Newton C (1969) Atmospheric circulation systems. Academic Press, 603 pp

Renfrew IA, Moore GWK, Clerk AA (1997) Binary interactions between polar lows. Tellus (Series A – dynamic meteorology and oceanography) 5(49): 577–594

Rithcie EA, Holland GJ (1993) On the interaction of tropical-cyclone scale vortices. II: Discrete vortex patches. Quart J Roy Meteor Soc 119: 1363–1379

Tafferner A (1990) Lee cyclogenesis resulting from the combined outbreak of cold air and PV against the Alps. Meteorol Atmos Phys 43: 31–47

Thorpe AJ (1985) Diagnosis of balanced vortex structure using potential vorticity. J Atmos Sci 42: 397–406

Ziv B, Alpert P (1994) Isobaric to isentropic interpolation errors and implication to PV analysis. J Appl Meteor 33: 694–703

Ziv B, Alpert P (1995) Rotation of binary cyclones – a data analysis study. J Atmos Sci 52: 1357–1369

Authors' addresses: Baruch Ziv (baruchz@openu.ac.il), The Open University of Israel, 16 Klousner St., Tel-Aviv 61392, Israel; Pinhas Alpert (e-mail: pinhas@cyclone.tau.ac.il), Department of Geophysics and Planetary Sciences, Raymond and Beverly Sackler Faculty of Exact Sciences, Tel Aviv University, Tel Aviv 69978, Israel.